# MEMO SPARK, no.3,2001

# CHOICE OF THE LINAC ENERGY WORKING POINT FOR THE FEL SPARK PROJECT

G. DATTOLI, L. GIANNESSI, L. PICARDI, P.L. OTTAVIANI, C. RONSIVALLE.

*In this memo we will discuss a criterion to obtain an operating point at fixed energy for the FEL operation at 13.5nm and 1.5nm*

The main problem to be solved in order to define a fixed energy working point of the LINAC for the FEL operation in the region around 13.5 nm and 1.5 nm is the necessity of finding a suitable condition for the matching of the LINAC performances to the requests imposed by the FEL. In other words the values of the beam energy spread, emittances and peak current at the chosen energy should be sufficient to guarantee the saturation of the laser at a reasonable undulator length and at a reasonable power.

The analysis so far developed using the two particle model developed in ref. (l) seems to confirm the possibility that one or more working point can be obtained.

Regarding the possibility of operating at two distinct energies, it has been pointed out that

a) the operation at 1 GeV and 13.5 nm can be achieved with the parameters summarized in Tab.l and fig.l

b) the operation at 2.5 GeV and 1.5 nm can be achieved with the parameters given in Tab.2 and fig.2

It is evident that in both cases we find "reasonable" solutions in the sense that saturation is reached with an undulator having a saturation length below 30 m and the brightness of the fundamental harmonic ranging around $10^{31}$.

This solution offers the possibility of using, for both operations, the same undulator, the different values of the K parameter can be obtained by adjusting the undulator gap.

Unfortunately the "modes" of operation at 1 and 2.5 GeV are not the same, since require different values of the $R_{56}$ matrix element for the compression dynamic, so that the system must be operated or at 1 GeV or at 2.5 GeV. (Fig.3)

An alternative scheme could be that of operating at the same energy with two different undulators.

A preliminary analysis has provided the following conclusions

i) the model of ref. (l) can be handled with just few minor changes (see Appendix) to obtain a working point at 1.8 GeV with an energy spread not exceeding $5 \cdot 10^{-4}$ (see fig.4)

ii) this value of energy, which is a compromise between 1 and 2.5 Ge V, can be exploited to fix two sets of undulator parameters for the operation in the wavelength region around 10nm and 1.5 nm.

The results are summarized in Tabs. 3,4 and figs. (5,6).

This analysis suggests that the system may operate at fixed energy with two different undulators (fig.7).

The advantages offered by this solution are evident:

l) More users can operate simultaneously

2) We have a definite economical advantage, which, also by taking into account the construction and the equipment of a second undulator, can be quantified on the order of 5GLit.

## L BAND operation

A second option is to combine a “cold” S band injector (up to 150 MeV) and a L band SC accelerator, in order to optimise the performances of the system. The application of the model outlined above (ref. 1 and Appendix) gives the results summarized in table 2a and in fig. 8. The energy spread at 1.8 GeV is $6 \cdot 10^{-4}$; if we do not include the wake fields it increases of a factor 2. In S band if we do not take into account the wake field the energy spread increase from $3 \cdot 10^{-4}$ to about $6 \cdot 10^{-3}$. As to the R56, in the S-band we can work with relatively low values of R56 (14 and 20

mm), while in the L band R56 increases respectively to 70 and 58 mm. This is only one of the possible solutions, considering the large number of free parameters (the values of intermediate energies and bunch lengths, the linac RF phases, the accelerating gradients).
Up to know in this analysis the effect on the emittance growth was not included, but if we take into account it, we see that it limits the number of free parameters.
In order to compare the S-band and the L-band operation we used the formulas of ref. 2 giving the emittance growth in magnetic compressors due two effects:

<u>Coherent synchrotron radiation</u> $\left(\frac{\Delta\varepsilon}{\varepsilon_0}\right)_{CSR} \propto \frac{N^2 \cdot |R_{56}|^{5/3}}{\varepsilon_N \cdot \sigma_z^{8/3}}$ (N= the number of particles in the bunch)

<u>Incoherent synchrotron radiation</u> $\left(\frac{\Delta\varepsilon}{\varepsilon_0}\right)_{ISR} \propto \frac{|R_{56}|^{5/2}}{\varepsilon_N} \cdot E^6$

*E(*GeV*),R56(*mm*),ε(*μm*)*

For the solution proposed in fig. 8 the ratio $\frac{\left(\frac{\Delta\varepsilon}{\varepsilon_0}\right)_{ISR}(Lband)}{\left(\frac{\Delta\varepsilon}{\varepsilon_0}\right)_{ISR}(Sband)}$ is 56 in BC1 and 50 in BC2 and

$\frac{\left(\frac{\Delta\varepsilon}{\varepsilon_0}\right)_{CSR}(Lband)}{\left(\frac{\Delta\varepsilon}{\varepsilon_0}\right)_{CSR}(Sband)}$ is 64 in BC1 and 6 in BC2.

It is evident that in order to reduce these high values it is necessary to decrease R56 and the values of intermediate energies at which the compression is performed. This was done in solution 2 (see table 3a and fig. 9) and we obtained $\frac{\left(\frac{\Delta\varepsilon}{\varepsilon_0}\right)_{ISR}(Lband)}{\left(\frac{\Delta\varepsilon}{\varepsilon_0}\right)_{ISR}(Sband)}$ of 1.6 in BC1 and 1.3 in BC2 and

$\frac{\left(\frac{\Delta\varepsilon}{\varepsilon_0}\right)_{CSR}(Lband)}{\left(\frac{\Delta\varepsilon}{\varepsilon_0}\right)_{CSR}(Sband)}$ of 4.6 in BC1 and 4.2 in BC2. The final energy spread is $3\ 10^{-4}$ and is obtained using a positive phase in the last linac. The wake fields are used but also if we consider null this effect the final energy spread is not larger that $10^{-3}$.

## Conclusions

The proposed solution based on the use of a fixed energy accelerator and two undulators seems to be attractive for many reasons, allowing in particular multi-users operation and reduced costs.
It requires a beam energy spread not larger than 0.1%: this value seems to be reachable both working in S band and L band from the simple model that has been used.
In both cases the energy spread compensation due to wake fields is used, but in L-band the wake fields is less effective. This could be an advantage for the L-band choice, because the wake field effect is not easily controllable, but the drawback is the use of higher values of R56 in the bunch compressor corresponding to an increase of emittance, that is another important parameter for FEL operation.

**REFERENCES**

(1) M. Ferrario, MEMO SPARK no. 2, 2001
(2) P. Emma "LCLS Accelerator Parameters and Tolerances for Low Charge Operations", LCLS-TN-99-3, May 3,1999

**Tables**

Table 1 parameters for operation at 1 GeV and 13.5 nm

| | #Harm. | 1st | 3rd | 5th |
|---|---|---|---|---|
| P | Power (W) | 3.5E+09 | 2.5E+08 | 3.0E+06 |
| e | Power density (MW/cm^2) | 1.8E+07 | 1.3E+06 | 1.6E+04 |
| a | Flux (Phot/sec/0.1%bw) | 1.1E+26 | 2.5E+24 | 1.8E+22 |
| k | Brightness ( Phot/sec/0.1% bw/mm/mrad) | 5.2E+30 | 1.2E+29 | 8.9E+26 |
| A | Power (W) | 1.2E+01 | 8.7E-01 | 1.1E-02 |
| v | Power density (MW/cm^2) | 6.4E-02 | 4.5E-03 | 5.5E-05 |
| e | Flux (Phot/sec/0.1%bw) | 3.8E+17 | 8.8E+15 | 6.4E+13 |
| r | Brightness ( Phot/sec/0.1% bw/mm/mrad) | 1.8E+22 | 4.3E+20 | 3.1E+18 |
| | Energy per pulse (mJ) | 3.5E+00 | 2.5E-01 | 3.0E-03 |
| | Photons per pulse /0.1% bw | 1.1E+14 | 2.5E+12 | 1.8E+10 |

Table 2 parameters for operation at 2.5 GeV and 1.5 nm

| | #Harm. | 1st | 3rd | 5th |
|---|---|---|---|---|
| P | Power (W) | 7.3E+09 | 2.0E+08 | 1.5E+07 |
| e | Power density (MW/cm^2) | 9.4E+07 | 2.7E+06 | 1.9E+05 |
| a | Flux (Phot/sec/0.1%bw) | 4.2E+25 | 3.9E+23 | 1.7E+22 |
| k | Brightness ( Phot/sec/0.1% bw/mm/mrad) | 1.3E+31 | 1.2E+29 | 5.1E+27 |
| A | Power (W) | 1.3E+01 | 3.6E-01 | 2.6E-02 |
| v | Power density (MW/cm^2) | 1.6E-01 | 4.6E-03 | 3.3E-04 |
| e | Flux (Phot/sec/0.1%bw) | 7.3E+16 | 6.9E+14 | 3.0E+13 |
| r | Brightness ( Phot/sec/0.1% bw/mm/mrad) | 2.2E+22 | 2.1E+20 | 8.9E+18 |
| | Energy per pulse (mJ) | 3.6E+00 | 1.0E-01 | 7.3E-03 |
| | Photons per pulse /0.1% bw | 2.1E+13 | 2.0E+11 | 8.4E+09 |

Table 3 parameters for operation at 1.8 GeV and 13.5 nm

| | #Harm. | 1st | 3rd | 5th |
|---|---|---|---|---|
| P | Power (W) | 3.5E+09 | 2.5E+08 | 3.0E+06 |
| e | Power density (MW/cm^2) | 1.8E+07 | 1.3E+06 | 1.6E+04 |
| a | Flux (Phot/sec/0.1%bw) | 1.1E+26 | 2.5E+24 | 1.8E+22 |
| k | Brightness ( Phot/sec/0.1% bw/mm/mrad) | 5.2E+30 | 1.2E+29 | 8.9E+26 |
| A | Power (W) | 1.2E+01 | 8.7E-01 | 1.1E-02 |
| v | Power density (MW/cm^2) | 6.4E-02 | 4.5E-03 | 5.5E-05 |
| e | Flux (Phot/sec/0.1%bw) | 3.8E+17 | 8.8E+15 | 6.4E+13 |
| r | Brightness ( Phot/sec/0.1% bw/mm/mrad) | 1.8E+22 | 4.3E+20 | 3.1E+18 |
| | Energy per pulse (mJ) | 3.5E+00 | 2.5E-01 | 3.0E-03 |
| | Photons per pulse /0.1% bw | 1.1E+14 | 2.5E+12 | 1.8E+10 |

Table 4 parameters for operation at 1.8 GeV and 1.5 nm

| | #Harm. | 1st | 3rd | 5th |
|---|---|---|---|---|
| P | Power (W) | 5.7E+09 | 1.1E+08 | 3.8E+05 |
| e | Power density (MW/cm^2) | 5.3E+07 | 1.0E+06 | 3.5E+03 |
| a | Flux (Phot/sec/0.1%bw) | 4.0E+25 | 2.5E+23 | 5.3E+20 |
| k | Brightness ( Phot/sec/0.1% bw/mm/mrad) | 6.2E+30 | 4.0E+28 | 8.3E+25 |
| A | Power (W) | 9.9E+00 | 1.9E-01 | 6.6E-04 |
| v | Power density (MW/cm^2) | 9.3E-02 | 1.8E-03 | 6.2E-06 |
| e | Flux (Phot/sec/0.1%bw) | 6.9E+16 | 4.4E+14 | 9.3E+11 |
| r | Brightness ( Phot/sec/0.1% bw/mm/mrad) | 1.1E+22 | 6.9E+19 | 1.5E+17 |
| | Energy per pulse (mJ) | 2.8E+00 | 5.4E-02 | 1.9E-04 |
| | Photons per pulse /0.1% bw | 2.0E+13 | 1.3E+11 | 2.7E+08 |

**Figures**

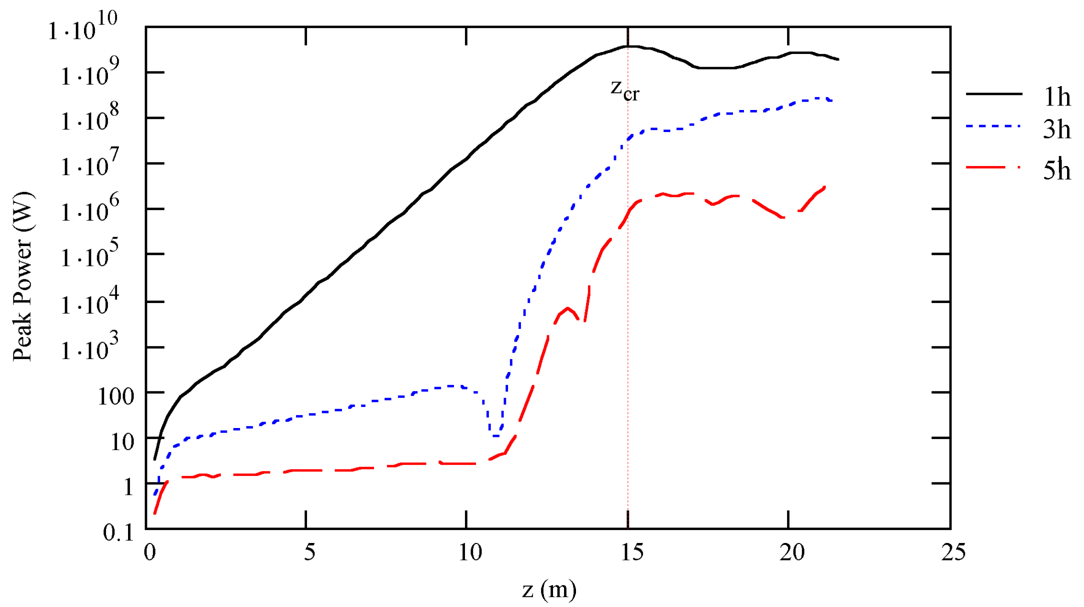


**Figure 1 FEL\ POWER vs z:1st ,2nd and 3rd harmonic, Energy 1GeV (parameters of Tab. 1)**

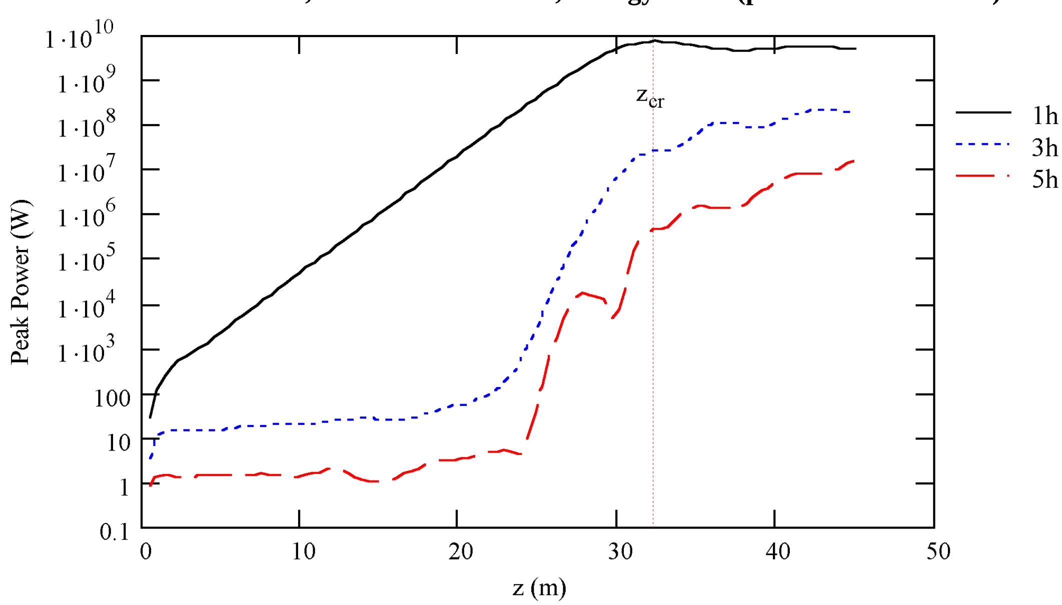


**Figure 2 Same as fig. 1, Energy 2.5 GeV (parameters of Tab.2)**

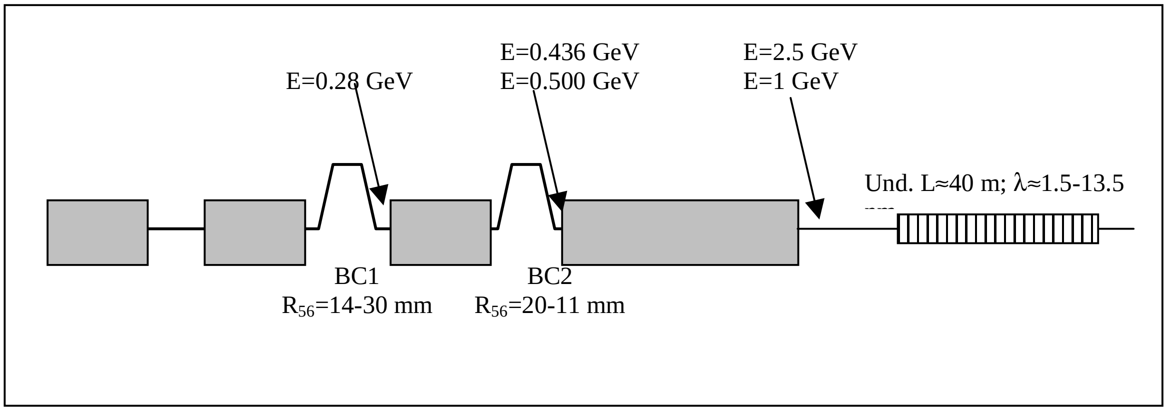


**Figure 3 FEL Operation with e-beam extraction at different energies**

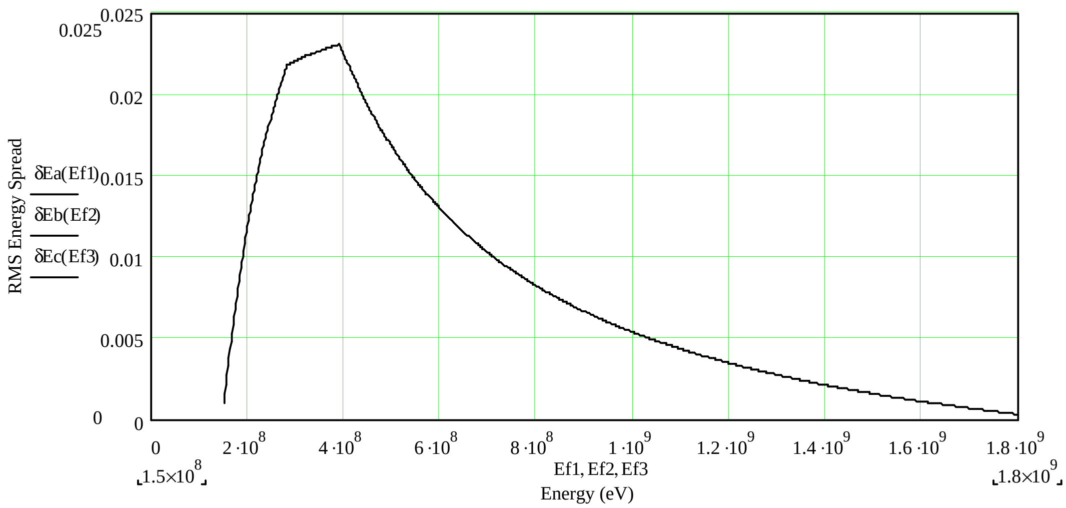


**Figure 4 ENERGY SPREAD vs ENERGY as predicted by the model of ref.(1) and Appendix (table 1a): S band operation**

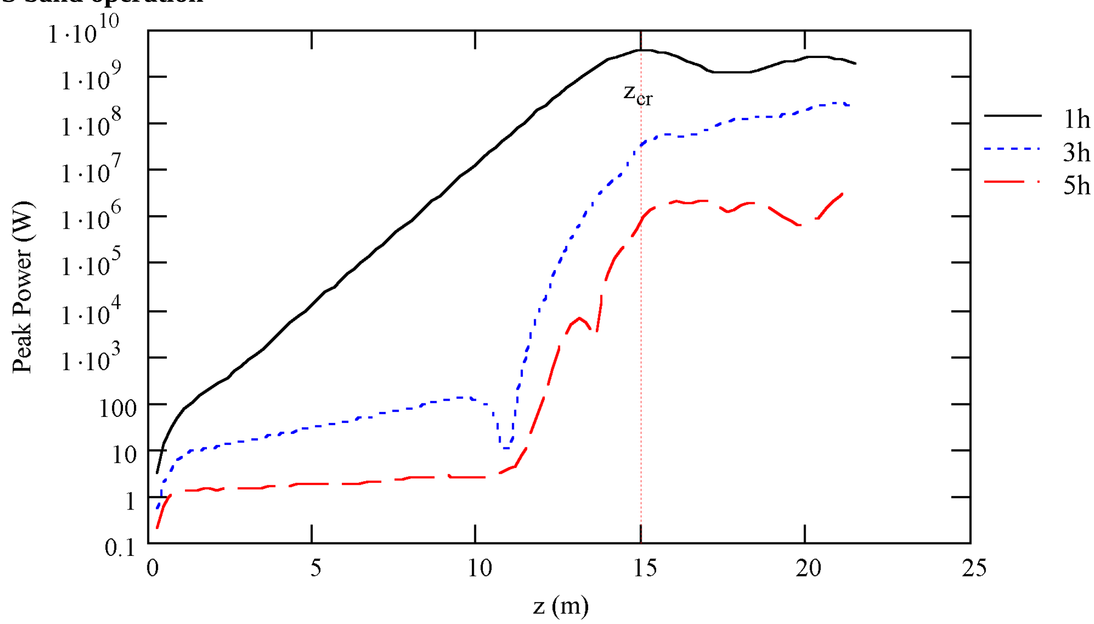


**Figure 5 Same as fig. 1): Energy 1.8 GeV (parameters of Tab. 3)**

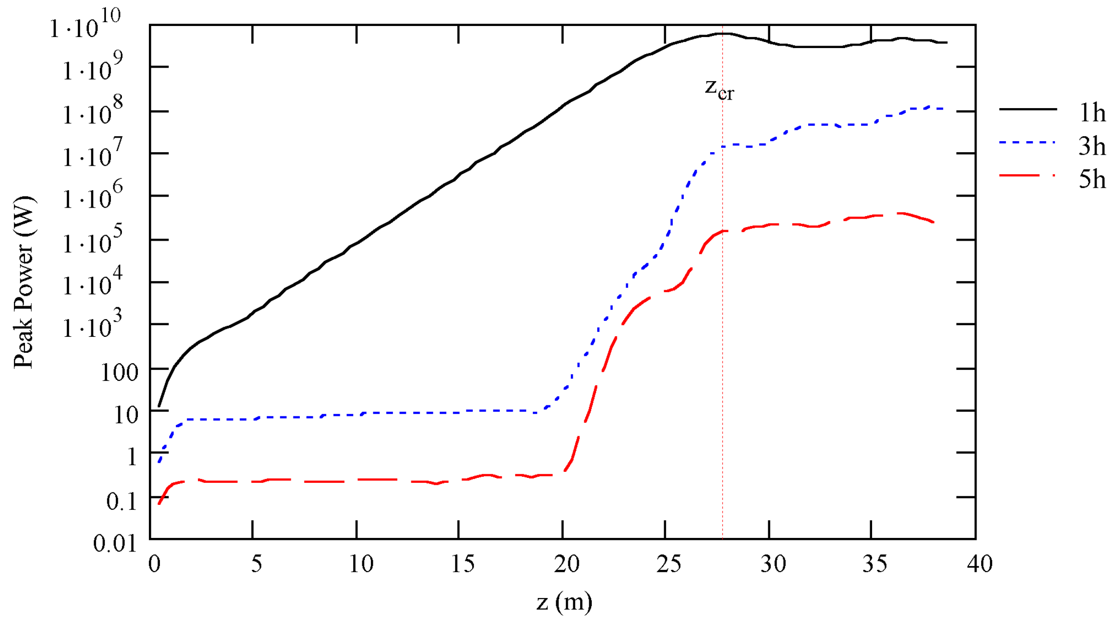


**Figure 6 - Same as fig. 1): Energy 1.8 GeV (parameters of Tab. 4)**

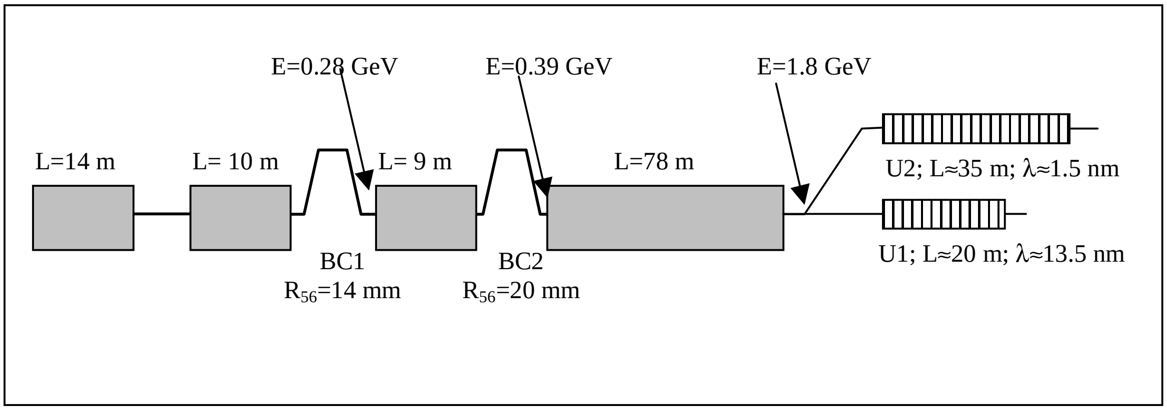


**Figure 7 FEL operation in S band with beam extraction at fixed energy.**

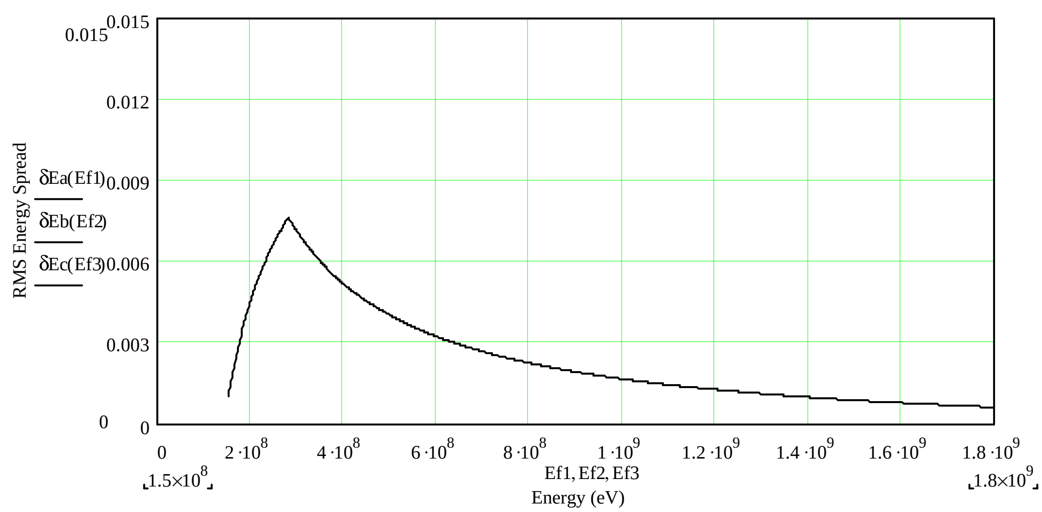


**Figure 8 ENERGY SPREAD vs ENERGY as predicted by the model of ref.(1) and Appendix (table 2a): L band operation. Solution 1.**

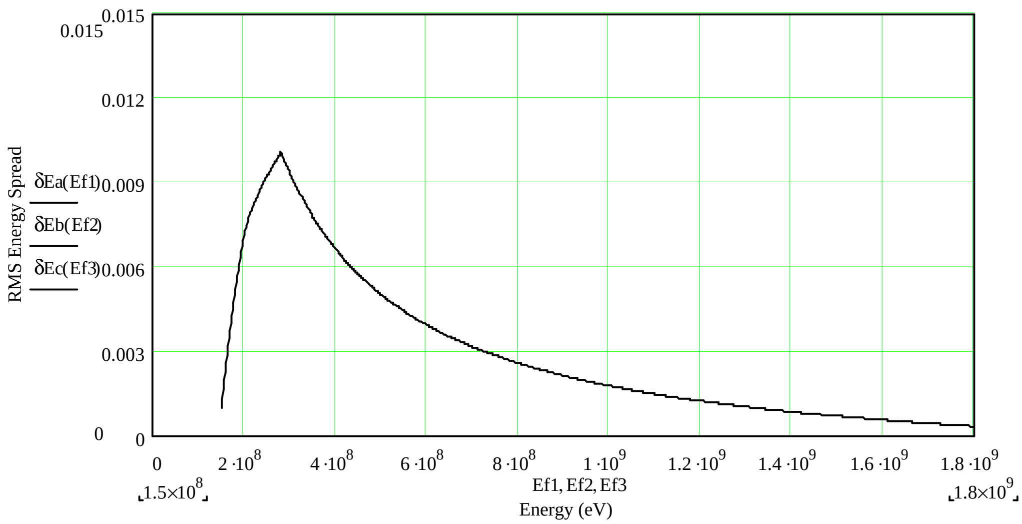


**Figure 9 ENERGY SPREAD vs ENERGY as predicted by the model of ref.(1) and Appendix (table 3a): L band operation. Solution 2.**

## APPENDIX

The beam energy spread after a nominal acceleration from $E_{i0}$ to $E_{f0}$ at an rf phase $\varphi_0$ (crest at $\varphi_0=0$ and $\varphi_0 \neq \pi/2$) is given by

$$\sigma_\delta = \frac{E_i - E_{i0}}{E_{f0}} - tg\varphi_0 \cdot k_{RF} \cdot \sigma_z \cdot \left(1 - \frac{E_{i0}}{E_{f0}}\right) - \frac{Q \cdot W_l(\sigma_z) \cdot (E_{f0} - E_{i0})}{2 \cdot E_{f0} \cdot \cos(\varphi_0) \cdot G} \qquad \text{(A.1)}$$

with $k_{RF} = \frac{2\pi}{\lambda}$ , $G$ = accelerating gradient , $\sigma_z$ = rms bunch length

$E_i$, $E_f$ = initial and final energy of a particle at an axial position $\sigma_z$

The first term is the initial energy spread scaled with the energy
The second term is the energy spread introduced by the linac section accelerating the beam with an off-crest rf phase for the following magnetic compression of the bunch
The third term is the energy spread due to longitudinal wake potential:

$$W_l(\sigma_z) = \frac{Z_0 \cdot c}{\pi \cdot a \cdot \sqrt{(a^2 + 8.6\sigma_z\lambda)}}$$

where a is the bore hole radius (a=12 mm at 2856 MHz, a=35 mm at 1300 MHz), Z0=377 ohm

The (A.1) was computed for the three parts in which the beam line following the 150 MeV injector is divided: LINAC1+first bunch compressor BC1, LINAC2+second bunch compressor BC2, LINAC3. The results are summarized in table 1a and in fig. 4.

Table 1a – Beamline parameters for 1.8 GeV operation (S band)

| Beamline | $E_{in}$ (GeV) | $E_{out}$ (GeV) | $\sigma_{-zin}$ (mm) | $\sigma_{-zout}$ (mm) | $\sigma_{-\delta in}$ (%) | $\sigma_{-\delta out}$ (%) | $\varphi_{RF}$ (deg) | Gradient (MV/m) | Length (m) | $R_{56}$ (mm) |
|---|---|---|---|---|---|---|---|---|---|---|
| LINAC1 | 0.15 | 0.28 | 0.83 | 0.83 | 0.1 | 2.2 | -45 | 18 | ≈ 10 | |
| BC1 | 0.28 | 0.28 | 0.83 | 0.52 | 2.2 | 2.2 | | | | 14 |
| LINAC2 | 0.28 | 0.39 | 0.52 | 0.52 | 2.2 | 2.3 | -45 | 18 | ≈ 9 | |
| BC2 | 0.39 | 0.39 | 0.52 | 0.055 | 2.3 | 2.3 | | | | 20 |
| LINAC3 | 0.39 | 1.8 | 0.055 | 0.055 | 2.3 | 0.03 | 0 | | ≈ 78 | |

*BC = magnetic bunch compressor*

Table 2a – Beamline parameters for 1.8 GeV operation (L band). Solution 1

| Beamline | $E_{in}$ (GeV) | $E_{out}$ (GeV) | $\sigma_{-zin}$ (mm) | $\sigma_{-zout}$ (mm) | $\sigma_{-\delta in}$ (%) | $\sigma_{-\delta out}$ (%) | $\varphi_{RF}$ (deg) | Gradient (MV/m) | Length (m) | $R_{56}$ (mm) |
|---|---|---|---|---|---|---|---|---|---|---|
| LINAC1 | 0.15 | 0.28 | 0.83 | 0.83 | 0.1 | 0.76 | -35 | 20 | ≈ 8 | |
| BC1 | 0.28 | 0.28 | 0.83 | 0.30 | 0.76 | 0.76 | | | | 70 |
| LINAC2 | 0.28 | 0.48 | 0.30 | 0.30 | 0.76 | 0.42 | 0 | 20 | ≈ 10 | |
| BC2 | 0.48 | 0.48 | 0.30 | 0.055 | 0.42 | 0.42 | | | | 58 |
| LINAC3 | 0.48 | 1.8 | 0.055 | 0.055 | 0.42 | 0.06 | 0 | | ≈ 66 | |

*BC = magnetic bunch compressor*

Table 3a – Beamline parameters for 1.8 GeV operation (L band). Solution 2

| Beamline | $E_{in}$ (GeV) | $E_{out}$ (GeV) | $\sigma_{-zin}$ (mm) | $\sigma_{-zout}$ (mm) | $\sigma_{-\delta in}$ (%) | $\sigma_{-\delta out}$ (%) | $\varphi_{RF}$ (deg) | Gradient (MV/m) | Length (m) | $R_{56}$ (mm) |
|---|---|---|---|---|---|---|---|---|---|---|
| LINAC1 | 0.15 | 0.2 | 0.83 | 0.83 | 0.1 | 0.73 | -50 | 20 | ≈ 4 | |
| BC1 | 0.2 | 0.2 | 0.83 | 0.55 | 0.73 | 0.73 | | | | 38.4 |
| LINAC2 | 0.2 | 0.28 | 0.55 | 0.55 | 0.73 | 1 | -50 | 20 | ≈ 6 | |
| BC2 | 0.28 | 0.28 | 0.55 | 0.055 | 1 | 1 | | | | 49.1 |
| LINAC3 | 0.28 | 1.8 | 0.055 | 0.055 | 1 | 0.03 | 25 | | ≈ 84 | |

*BC = magnetic bunch compressor*